Biogeosciences Discuss., 10, 8977–9002, 2013
www.biogeosciences-discuss.net/10/8977/2013/
doi:10.5194/bgd-10-8977-2013

Biogeosciences Discussions Open Access

Authigenic phases and biomass contents drive Zr, Hf and REE distributions in anoxic lake sediments

P. Censi[1,2], F. Saiano[3], P. Zuddas[4], A. Nicosia[2], S. Mazzola[2], and M. Raso[1]

[1]DISTEM department, Università di Palermo, Via Archirafi, 22, 90123 Palermo, Italy
[2]IAMC-CNR, UOS Capo Granitola, via del Mare, 3, 91021 Campobello di Mazara, Italy
[3]SAF department, Università di Palermo, Viale delle Scienze, 13, 90128 Palermo, Italy
[4]Université Pierre et Marie Curie, Paris 6 Institut des Sciences de la Terre 4, place Jussieu F75005 Paris, France

Received: 3 April 2013 – Accepted: 12 May 2013 – Published: 31 May 2013

Correspondence to: P. Censi (paolo.censi@unipa.it)

Published by Copernicus Publications on behalf of the European Geosciences Union.

Abstract

REE, Zr and Hf distributions in seafloor sediments collected from the hypersaline, anoxic Thetis, Kryos, Medee and Tyro deep-sea basins from the Eastern Mediterranean were determined in light of their mineralogical composition, and biomass contents. Mineralogical investigations demonstrate that all the studied sediments show a similar mineralogy. Detritic assemblages mainly consist of quartz, gypsum and calcite with Mg contents ranging from 0 to about 7 %, often of a bioclastic nature. On the contrary, authigenic parageneses are formed by halite, bischofite, dolomite and calcite, with Mg contents up to 22 %. Textural evidences of biological activity were also identified. In sediments from the Medee and Tyro basins, REE, Zr and Hf distributions were analysed in the fraction soluble in nitric acid, whereas in materials coming from the Thetis and Kryos basins, the water-soluble sediment fraction had been previously removed and REE, Zr and Hf distributions were investigated in the residue. This approach evidenced that shale-normalised REE patterns of the whole fraction soluble in nitric acid show strong intermediate REE (MREE) enrichments that give way to positive Gd anomalies once water-soluble minerals are removed.

Y/Ho ratios are clustered around chondritic values justified by the occurrence of detritic minerals whereas Zr/Hf values span a wider range from slightly subchondritic to superchondritic terms. Negative Gd anomalies, subchondritic Y/Ho and Zr/Hf values are found in Mg-carbonate rich samples suggesting that authigenic Mg-carbonates partition Ho and Hf with respect to Y and Zr during their crystallization from brines. Textural observations and biomass analyses highlighted effects of biological activities in sediments involving Zr and Hf enrichments and the highest Zr/Hf values according to the preferential Zr removal onto biological surfaces, without partitioning Y with respect to Ho. These first data suggest that Zr/Hf ratio and REE distributions can represent tracers of biological activity in sediments.

BGD
10, 8977–9002, 2013

1 Introduction

The geochemical significance of studies carried out on marine sediments based on trace metal distributions is mainly limited by the simultaneous occurrence of more or less complicated authigenic fractions associated with a wide range of detritic minerals. This evidence implies that a deep knowledge of the mineralogical composition of the sediments and their textures in terms of the distribution of studied metals in these sediments is hard to achieve.

In particular, in extreme sedimentary environments, such as those occurring in hypersaline anoxic lakes underlying the oxic water column in the Eastern Mediterranean basin, these problems are further complicated by the occurrence of halides and primary Mg-rich carbonates that crystallize under the extreme conditions occurring in these environments. The capacity to recognise the geochemical significance of trace element distributions in these materials is worsened by the paucity of data about natural examples of the occurrence of these minerals and the processes occurring during their crystallization (Pierre et al., 1984; Sanz-Montero et al., 2008, 2009; Last et al., 2012). At the same time, limited information has been reported regarding the origin of dissolved trace elements in these environments and the processes allowing their partitioning during solid-liquid processes (Saager et al., 1993; Schijf et al., 1995; Bau et al., 1997). Moreover, significant biological activity also occurs in these extreme environments (Pikuta et al., 2002; Sass et al., 2002; Torfstein et al., 2005; Yakimov et al., 2007; Borin et al., 2009; La Cono et al., 2011; Smedile et al., 2012), representing a further aspect that can influence trace element behaviour during the competition between dissolved complexation and scavenging onto surfaces of biological membranes, as demonstrated during in-field and in-lab observations (Takahashi et al., 2005, 2007, 2010).

The ensemble of these processes complicates the possibility of attributing a geochemical significance to measured trace element distributions under these conditions. In this study the possibility that this difficulty can be overwhelmed coupling

BGD
10, 8977–9002, 2013

quantitative determinations of trace element with recognition of mineralogical compositions biomass contents and textures determinations in sediments is suggested. Moreover, trace metal distributions among detritic minerals, authigenic phases and organic substance/biological matter responsible for metal behaviour in sediments, as processes dominated by interface reactions usually leading to elemental fractionations, can be deeply investigated by means of REE (lanthanides and yttrium) behaviour, which has been demonstrated to represent a powerful tracer for investigating these phenomena (Haley et al., 2004). These considerations have never, to the authors' knowledge, been addressed in a single study associated with the study of Zr–Hf relationships, in spite of the fact that this geochemical twin can also represent another promising indicator of processes involving elemental fractionation at solid-liquid and organic-inorganic interfaces. Following this suggestion, the aim of this work is to improve the boundary of geochemical knowledge of processes allowing fractionation of REE, Zr and Hf during the crystallization of carbonates and Na- and Mg-halides, about which there is very little data, in order to contribute to enlarging our recognition of and knowledge about these processes occurring at solid-liquid interfaces through their effects on the simultaneous behaviour of REE, Zr and Hf.

2 Materials and methods

The studied sediments were collected in the Eastern Mediterranean Sea during the oceanic cruise MAMBA 2010, carried out with RV Urania by M. Yakimov's team from the Italian National Research Council, IAMC section of Messina (Italy). Sample collections were carried out on the seafloor of hypersaline lakes occurring in the Medee, Tyro, Thetis and Kryos basins in the Eastern Mediterranean Sea close to Crete (Fig. 1). The investigated basins are located in the inner portion of the so-called "Mediterranean ridge accretionary complex" (Bortoluzzi et al., 2011), in the eastern basin where the occurrence of a particular seafloor topography is also associated with the presence of Messinian evaporites lying immediately below thin hemipelagic sediments (Ryan et al.,

BGD
10, 8977–9002, 2013

1973; Hsu and Mortadert, 1978). This allowed the formation of deep lakes filled by hypersaline brines. According to Camerlenghi (1990), the tectonic deformation of seafloor sediments coupled with the submarine dissolution of Messinian evaporitic sediments (Cita, 2006) enabled the formation of the basins and related hypersaline lakes filled therein. Bortoluzzi et al. (2011) described sediments from the Kryos, Thetis and Medee basins as sandy products underlying to a basal layer of grey mud about 23 cm below the seafloor that they interpreted as turbidites from the flanks of ridges probably fallen as a consequence of tectonic activity. Rimoldi and Cita (2007) investigated sediments from the Tyro basin and recognised a deep sequence of homogeneous green mud, rich in organic matter, that was trigged by seismic events and/or tectonically induced tsunamis.

Sample collections of sediments were carried out employing an USGS-modified NEL-box corer (Tranchida et al., 2011). After collection, the samples were stored in polyethylene liners and kept frozen (at −20 °C) until chemical analysis. In the laboratory, the defrosted cores were cut at 1–2 cm intervals with a stainless steel band saw and dried at 50 °C. Samples from the Thetis and Kryos basins had previously been ultrasonically cleaned in high-purity water (18.2 $M\Omega\,cm^{-1}$) in order to remove salt minerals, whereas those coming from the Tyro and Medee basins were analysed without further manipulations.

X-Ray investigations were carried out using a Philips PW14 1373 X-ray spectrometer employing a Cu-Kα radiation (2Θ range 3–90°, step size 0.02°, step time 1 min) and refined by the Rietveld method (Program DiffracPlus TOPAS®. Version 4.0, Bruker AXS Inc., Karlsruhe, Germany, 2004). This method consists of a fitting between the experimental XRD spectrum of the investigated sample and a theoretical spectrum calculated by means of several structural parameters by least squares method refinement (Young, 1993). Starting parameters for the Rietveld refinement method were obtained from the Inorganic Crystal Structure Database (ICSD) program. The calculation of $MgCO_3$ contents was carried out according to the experimental curve reported by Zhang et al. (2012). In order to carry out scanning electron microscopic (SEM)

BGD
10, 8977–9002, 2013

investigations, sediment samples were previously dried at 105 °C, coarsely crushed in an agate mortar, mounted on aluminium stubs and then carbon coated. SEM analyses were carried out using a LEO 440 SEM equipped with an EDS system OXFORD ISIS Link and Si (Li) PENTAFET detector.

Chemical analyses were carried out by digesting 100 mg of each sample in 10 mL of a 1 : 1 HNO_3-H_2O_2 mixture in a Teflon TFM sealed bomb using a microwave mineralizer (CEM MARS 5 device). Thereafter, with sediments from the Thetis and Kryos basins, the trace element composition of the sediment fraction free from water-soluble salts (hereafter defined FWSS) was investigated, whereas the whole sediment composition (hereafter defined WS) was studied in the Medee and Tyro samples. Based on the mineralization procedure used, only trace elements coming from the dissolution of carbonates, sulphates, sulphides and organic matter were collected and investigated, whereas silicate residue was separated from the dissolved phase after filtration onto previously acid-cleaned 0.45 µm Millipore™ filters. After filtration the obtained solution was diluted to a 50 mL volume and stored for chemical analyses. These analyses were carried out by inductively coupled plasma mass spectrometry (ICP-MS) using an Agilent Technologies 7500ce Series Spectrometer equipped with a collision cell. All instrumental parameters were optimized daily using a 1 ng mL^{-1} solution of ^{7}Li, ^{89}Y, ^{140}Ce, ^{205}Tl; to obtain maximum sensitivity the instrument was tuned on ^{89}Y. Each solution was measured three times and ICP-MS analyses were carried out with a classical external calibration approach. Such an approach involved investigating a range of concentrations for each element between 2.5 and 500 pg mL^{-1}, and using ^{205}Tl (1 ng mL^{-1}) as an internal standard to compensate for any signal instability or sensitivity changes during the analysis. A 1 M HCl blank was run during the analysis to ensure that the memory effect, due to the more refractory elements, was negligible.

During sample manipulations and analyses only ultrapure reagents were used. High purity water, 18.2 M cm, was obtained by the Easy Pure II purification system (Thermo, Italy). Ultra clean acids (nitric, hydrochloric acid and hydrogen peroxide) used for sample analysis and cleaning plasticware were purchased from BAKER chemicals (Baker

BGD
10, 8977–9002, 2013

Ultrex II®). Working standard solutions for each element (Zr, Y, La, Ce, Pr, Nd, Sm, Eu, Gd, Tb, Dy, Ho, Er, Tm, Yb, Lu and Hf) were prepared daily by stepwise dilution of multi-element stock standard solutions from CPI International™ ($1000 \pm 5\,\mu g\,mL^{-1}$) in a HCl medium.

DNA, as a robust indicator of soil microbial biomass (Marstorp et al., 2000; Dequiedt et al., 2011), was extracted from sediments using a modified procedure previously described by Ranjard et al. (Ranjard et al., 2003). Equal amount of samples (0.5 g, dry weight) was frozen in liquid N_2 and mixed with 700 mg and 150 mg of 106 mm and 2 mm diameter glass beads respectively. Samples were grinded for 1 min. at 2000 r.p.m. in a mini bead-beater cell disruptor (Mikro-dismembrator S.B. Braun Biotech International, Melsungen, Germany). The obtained fine powder were then resuspended in 1.5 mL of a pre-warmed (70 °C) lysis solution containing 100 mM Tris-HCl (pH 8.0), 100 mM EDTA; (pH 8.0), 100 mM NaCl and 2 % (w/v) SDS, then transferred to 10 mL conical tube. Samples were incubated in an hybridization oven, ensuring continuous and gentle rotation, for 30 min at 70 °C and then centrifuged at 7000 g for 5 min. at 10 °C. Supernatants were recovered, precipitated with 1/10 volume of 3 M CH_3COOK (pH 5.5) and one volume of ice-cold isopropanol, then centrifuged at 14 000 rpm for 5′. The nucleic acids were washed with 70 % ethanol and resuspended in 80 µL of sterile ultrapure water. Each extraction was repeated in triplicate.

Purified DNA extracts were fluorometrically quantified using Qubit® 2.0 (Life Technologies Corporation, Carlsbad, USA) following manufacturer's instruction. DNA quantifications were confirmed by electrophoresis on 0.7 % agarose gels stained with SYBR® Safe (Life Technologies Corporation, Carlsbad, USA). Serial dilutions of Salmon Sperm DNA Solution (Life Technologies Corporation, Carlsbad, USA) were added in each gel as a standard curve to estimate the DNA concentration in each sample. Agarose gels were captured using VersaDoc system and the Quantity One software (Bio-Rad Laboratories, Hercules, CA, USA) was used for densitometric analysis.

BGD
10, 8977–9002, 2013

3 Results

3.1 Mineralogy

X-Ray analyses evidenced a monotonous mineralogical composition in the investigated sites (Supplement 1). In all the studied samples, calcite, Mg-calcite, dolomite and quartz were recognised. Soluble salt minerals (halite and bischofite) were found only in sediments from the Medee and Tyro basins, having been removed from the Thetis and Kryos sediments during manipulation procedures. Analyses of the peak shape of the calcite d(104) XRD effect showed a significant grade of asymmetry in the effect, suggesting the presence of different calcite generations (Milliman et al., 1971): (i) Mg-free calcite with d(104) close to 3.030 Å, (ii) low-Mg calcite with d(104) values close to 3.013 Å (corresponding to a $MgCO_3$ molar content close to 8 %) and (iii) high-Mg Calcite with d(104) values close to 3.001 Å (corresponding to a $MgCO_3$ molar content close to 12 %). X-ray results are in agreement with SEM observations that show a significant mineral assemblage of detritic origin consisting of bioclastic products (Fig. 2a, b), carbonate lithic fragments (Fig. 2c) and gypsum crystals (Fig. 2d), probably from evaporitic terrains of the Miocene Age, and rounded quartz (Fig. 2e). Authigenic carbonates mainly consist of high-Mg calcite and dolomite (Fig. 2f), sometimes containing Fe and Mg-calcite microcrysts are often spanned in sediment assemblages mixed with detrital components. Soluble salt minerals, consisting of abundant halite and bischofite crystals, characterize the shallowest sediment layers and often encrust bioclasts (Fig. 2g). Furthermore, SEM images provide evidence of fibrous materials, probably related to the presence of a microbial mat/organic fraction in the sediments (Fig. 2h, i), in agreement with results of recent microbiological studies (Ferrer et al., 2012; Stock et al., 2012) and sedimentological investigations (Rimoldi and Cita, 2007).

In the Medee basin, deep sediments from below 25 cm depth, show large amounts of low-Mg calcite from foraminifera shells, up to 90 %. In shallowest sediments, detritic phases (Mg-free calcite, low-Mg bioclastic calcite and quartz) decrease up to around 50 %. High contents of low-Mg calcite from bioclastic origin are also found in studied

BGD
10, 8977–9002, 2013

specimens from Thetis and Kryos sequences. In Tyro sediments the amplitude of detritic minerals is lower with respect to other studied sediments (about 40 %), especially in samples from depths of 4–6 cm and 10–11 cm where halides and high-Mg calcite and dolomite are more concentrated.

3.2 Geochemistry

REE, Zr and Hf concentrations measured in sediments are reported in Supplement 1. The recognised concentrations are always higher in Tyro and Medee sediments, with mean REE values ranging from 70 ± 7.9 ppm and 72.6 ± 7.9 ppm, respectively. Similarly, Zr and Hf mean contents range from 47.25 ± 9 and 46.28 ± 9.7 ppm (Zr) and from 1.05 ± 0.15 and 0.89 ± 0.17 ppm (Hf) in Tyro and Medee sediments, respectively. By contrast, lower values were found in Kryos and Thetis sediments, where mean REE concentrations range from 32.55 ± 3.7 to 45.2 ± 7.7 ppm, respectively. Mean Zr values changed from 7.33 ± 1.2 to 9.32 ± 2.5 ppm in Kryos and Thetis sediments, respectively, whereas mean Hf values are close to 0.35 ± 0.08 ppm in both sediment sequences. These differences indicate that the investigated trace elements are concentrated both in soluble halides and in minerals forming FWSS. As a consequence, sediments from the Tyro and Medee basins show higher concentrations because soluble halides were not previously removed from the mineralized sediments during analytical procedures.

Although REEs are distributed in both fractions, features of shale-normalised patterns vs. PAAS (Taylor and McLennan, 1995) are different in WS (Tyro and Medee) with respect to FWSS (Kryos and Thetis) samples. These differences mainly regard distributions of intermediate REE (MREE) that are variably enriched with respect to light REE (LREE) and heavy REE (HREE). In shale-normalised patterns of WS sediments a progressive MREE enrichment from Eu to Ho is observed, followed by a progressive HREE depletion along the series. On the contrary in FWSS sediments MREE enrichments are less noticeable with significant positive Gd anomaly, as defined by Moller

BGD
10, 8977–9002, 2013

et al. (2007):

$$\frac{Gd}{Gd^*} = \frac{Gd_n \sqrt{Ho_n}}{\sqrt{Tb_n^3}} \quad (1)$$

Therefore, measured Gd/Gd* values represent a characteristic feature to discriminate samples coming from the Tyro and Medee basins, characterised by negative or slightly positive Gd anomalies, from sediments collected in seafloor from the Thetis and Kryos saline lakes, where positive Gd anomalies have been measured (Fig. 3).

In the light of mineralogical compositions of studied sediments, shale-normalised REE features suggest that a positive Gd anomaly is a characteristic of FWSS where mainly occur carbonates of different origin and sulphur-bearing components coming from Kryos and Thetis sediments where soluble salts and partially organic substances where removed during sample manipulations. In contrast, the MREE bulge distributions observed in REE patterns of sediments collected in the Tyro and Medee basins are similar to REE features shown by estuarine Fe- and organic-rich sediments and attributed to the occurrence of reactive Fe-sulphide species and/or organic matter (Morgan et al., 2012). In Tyro and Medee sediments the positive relationship between normalised MREE/HREE concentrations and the amount of biomass suggest that the amount of organic material dispersed in Tyro and Medee sediments can play a major role in the observed MREE enrichment of these materials (Fig. 4).

Y/Ho values of studied sediments fall between about 30 and 55 (molar ratios) and are inversely related to contents of Mg-carbonates (calcite + dolomite) in sediments from Medee and Tyro sequences (R_{xy} = 0.92; $t_{\alpha/2}$ = 13.7; $\alpha < 0.025$) as reported in Fig. 5a. Here, samples with high-Mg calcite and dolomite contents show subchondritic Y/Ho values, whereas samples rich in bioclastic carbonates and other detritic phases are clustered close to chondritic values. This evidence suggests a preferential Ho partitioning in solids with respect to Y during authigenic carbonate crystallizations, in agreement with experimental evidence (Qu et al., 2009). Figure 5b show that Zr/Hf ratios similarly

BGD
10, 8977–9002, 2013

behave with respect to Mg-carbonate content in sediments (R_{xy} = 0.72; $t_{\alpha/2}$ = 5.98; $\alpha < 0.025$), suggesting that the crystallization of Mg-carbonates influences both Y–Ho and Zr–Hf fractionations under natural conditions as well as in lab experiments (Qu et al., 2009). At the same time Y/Ho and Zr/Hf ratios are related to the biomass content in Tyro and Medee sediments (Fig. 6) suggesting that biological materials can influence the reciprocal behaviour of these elements.

4 Discussion

According to the above-mentioned evidences, lower trace element concentrations, positive Gd anomalies, subchondritic Y/Ho and Zr/Hf values and the removal of water-soluble minerals characterise FWSS samples collected in the Thetis and Kryos seafloor basins. $Gd/Gd^* > 1$ values recognised in these samples agree with the occurrence of low-Mg calcite from foraminifera shells similarly as occurs in recent biogenic carbonates and differently with respect to Gd/Gd^* values measured in fossil carbonates (Azmy et al., 2011). This process is consistent with the REE^{3+} capability to substitute for Ca^{2+} in several minerals, including calcite (Zhong and Mucci, 1995), especially when this process is coupled with the incorporation of Na^+ at Ca^{2+} sites in order to balance the excess charge created by the coprecipitation of REE^{3+}. The geochemical behaviour of Y and Ho during the crystallization of biogenic calcite from seawater is not known. Therefore subchondritic Y/Ho values recognised in sediments enriched in low-Mg bioclastic calcite from Thetis and Kryos basins (Supplement 1) suggest that Ho is preferentially partitioned in calcite with respect to Y also in biogenic carbonates (Tanaka and Kawabe, 2006; Qu et al., 2009). Coupled recognition of subchondritic values also for Zr/Hf ratio in Thetis and Kryos sediments suggests that also Hf can be partitioned in biogenic calcite with respect to Zr, although the only Zr/Hf values known are related to carbonatites where Zr/Hf values can be affected by different dissolved complexation behaviour of these elements in supercritical carbonatitic fluids.

BGD
10, 8977–9002, 2013

Large MREE enrichments coupled with chondritic and superchondritic Y/Ho and Zr/Hf values, respectively, have been measured in sediments where the WS fraction has been considered and higher trace element contents are reached. In these sediments significant concentrations of authigenic carbonates (Mg-rich calcite and dolomite) and soluble salts associated with variable amounts of detritic phases (Supplement 1) suggests that these minerals crystallizing from brines are less affected by Gd enrichments with respect to bioclastic low-Mg calcite from Kryos and Thetis sediments. This hypothesis is confirmed by REE features recognised in authigenic aragonite samples (Himmler et al., 2010) and vein dolomites (Kučera et al., 2009) characterised by MREE enrichments and slight Gd depletions, associated with Y/Ho values from subchondritic to chondritic, respectively.

If authigenic Mg-calcite and dolomite are slightly depleted in Gd, also soluble halite and bischofite salts should be Gd-depleted in order to justify the observed Gd-enriched brines associated (Censi et al., 2013) and positive Gd anomalies recognised in seawater and lacustrine brines from several areas and contexts worldwide (Fee et al., 1992; Bau et al., 1997; De Carlo and Green, 2002; Gavrieli and Halicz, 2002; Moller et al., 2007). Therefore, a further sediment component should be invoked to justify Gd/Gd^* close to 1 or slightly higher observed in Tyro and Medee samples. This component should have $Gd/Gd^* \geq 1$, MREE enrichment chondritic or slight higher Y/Ho values and Zr/Hf ratios from chondritic to superchondritic in order to agree with values recognised in studied sediments from Medee and Tyro basins. We suggest that this component is organic matter associated to bacterial colonies recognised during this study and previous investigations (Rimoldi and Cita, 2007). In order to support this hypothesis investigated samples have been depicted according to their Y/Ho vs. Zr/Hf values (Fig. 7). These values describe an almost horizontal trend for Y/Ho values clustered around the chondrite interval ($Y/Ho \approx 52$) or slightly higher that progressively evolves along a hyperbolic path (trend "a" in Fig. 7). As previously mentioned, the lowest Y/Ho and Zr/Hf values falling on this array are measured in WS samples from the Tyro basin, where authigenic Mg-carbonates are associated with high halide and lower detritic mineral

BGD
10, 8977–9002, 2013

contents. The observed co-variant Y/Ho vs. Zr/Hf values in these sediments were previously recognised in primary carbonatites (Alberti et al., 1999; Bizimis et al., 2003) and explained by liquid immiscibility during magmatic differentiation processes (Brod et al., 2013).

In contrast, the higher affinity of Zr and Hf for organic surfaces with respect to REE and other metals (Monji et al., 2008), coupled with the lack of fractionation between Y and Ho under bacterial surfaces that allows the "chondritic" Y/Ho signature of these materials (Takahashi et al., 2005) could explain the observed sub-horizontal behaviour of the hyperbolic trend and the observed chondritic Y/Ho threshold recognised in studied sediments from the Medee and Tyro basins. In these samples high Y/Ho and Zr/Hf values are related with the biomass contents (Fig. 4) whereas MREE enrichments represent a further evidence of suggested preferential MREE partitioning onto organic surfaces where carboxyl and polyphosphate groups bind REE subtraction them from dissolved pool (Takahashi et al., 2007, 2010).

On the other side FWSS sediments from the Thetis and Kryos basins describe an extension of hyperbolic trend "a" towards subchondritic Y/Ho and Zr/Hf values (trend "b"). The similar shapes of these trends may originate from the removal of the water-soluble fraction from the Thetis and Kryos samples. This process could allow Zr/Hf subchondritic values in Thetis and Kryos samples if halides are characterised by superchondritic Zr/Hf values, as suggested by the composition of Tyro and Medee sediments. Accordingly, Zr–Hf decoupling in aqueous solutions is driven by alkalinity, insomuch as fractional crystallisation of carbonates has been the historical method to separate these elements (Gmelin, 1941). Therefore, brines with higher Zr/Hf ratios and consequent crystallization of authigenic halide minerals with superchondritic Zr/Hf ratios are expected.

BGD
10, 8977–9002, 2013

5 Conclusions

Geochemical investigations carried out on sediments coming from deep-sea hypersaline basins in the Eastern Mediterranean indicate that features observed in REE, Zr and Hf distributions are mainly influenced by competitions between dissolved complexation and surface complexation onto authigenic crystallizing minerals or REE, and other investigated elements can be incorporated by substituting for major ions in the crystal structures of authigenic minerals. Further effects induced by occurrences of organic matter/biological activity are suggested by Zr–Hf fractionation, in contrast with the coherent behaviour of Y and Ho. As regards the Gd anomaly, the crystallization of authigenic Mg-rich carbonates involving the development of positive Gd anomalies in the studied assemblages strongly suggests preferential Gd partitioning in these minerals with respect to its neighbours along the REE series. This process would lead to a Gd-depleted mother brine. The crystallization of authigenic halides from this brine produces Gd depleted halite and bischofite and moderate positive anomalies in the residual dissolved phase. This scenario is consistent with observed Gd enrichments in several hypersaline lakes in different environments. The exploitation of the reciprocal behaviour of Y–Ho and Zr–Hf isovalent geochemical twins as geochemical proxies of interface processes represents the best approach to depicting the whole process allowing crystallization of authigenic minerals in sedimentary assemblages where detritic minerals occur widely. This evidence is validated by the behaviour of investigated sediments that fall along two mixing arrays due to the progressive growth of crystallizing Mg-rich carbonates with or without halides, respectively.

In this scenario, the effects of microbial activity can play a role in determining further enrichment in Zr and Hf in sedimentary assemblages and producing the observed lack of fractionation between Y and Ho that enables the observed chondritic Y/Ho signature in many studied samples. These are the first data about effects induced by the crystallization of halides and other soluble phases on REE, Zr and Hf distributions in saline systems between newly forming salt minerals and dissolved media. Therefore

BGD
10, 8977–9002, 2013

further researches are required focused on analogous saline Mediterranean sediments in more accessible areas where saline minerals are forming

Supplementary material related to this article is available online at: http://www.biogeosciences-discuss.net/10/8977/2013/bgd-10-8977-2013-supplement.pdf.

Acknowledgements. We are indebted to M. Yakimov and his team for facilities offered to the authors during the Mamba 2010 oceanographic cruise and to G. Tranchida, E. Oliveri and M. Sprovieri who allowed us to investigate sediment samples collected during the cruise.

References

Alberti, A., Castorina, F., Censi, P., Comin-Chiaramonti, P., and Gomes, C. B.: Geochemical characteristics of Cretaceous carbonatites from Angola, J. Afr. Earth. Sci., 29, 735–759, 1999.

Azmy, K., Brand, U., Sylvester, P., Gleeson, S. A., Logan, A., and Bitner, M. A.: Biogenic and abiogenic low-Mg calcite (bLMC and aLMC): Evaluation of seawater-REE composition, water masses and carbonate diagenesis, Chem. Geol., 280, 180–190, 2011.

Bau, M., Moller, P., and Dulski, P.: Yttrium and lanthanides in eastern Mediterranean seawater and their fractionation during redox-cycling, Mar. Chem., 56, 123–131, 1997.

Bizimis, M., Salters, V. J. M., and Dawson, J. B.: The brevity of carbonatite sources in the mantle: evidence from Hf isotopes, Contrib. Mineral. Petr., 145, 281–300, 2003.

Borin, S., Brusetti, L., Mapelli, F., D'Auria, G., Brusa, T., Marzorati, M., Rizzi, A., Yakimov, M., Marty, D., De Lange, G. J., Van Der Wielen, P., Bolhuis, H., McGenity, T. J., Polymenakou, P. N., Malinverno, E., Giuliano, L., Corselli, C., and Daffonchio, D.: Sulfur cycling and methanogenesis primarily drive microbial colonization of the highly sulfidic Urania deep hypersaline basin, P. Natl. Acad. Sci. USA, 106, 9151–9156, 2009.

Bortoluzzi, G., Borghini, M., La Cono, V., Genovese, L., Foraci, F., Polonia, A., Riminucci, F., Marozzi, G., and Yakimov, M.: The exploration of deep anoxic basins of the earstern Mediter-

BGD
10, 8977–9002, 2013

ranean sea, in: Marine Reasearch at CNR, Italian Consiglio Nazionale delle Ricerche, Italy, 2011.
Brod, J. A., Junqueira-Brod, T. C., Gaspar, J. C., Petrinovic, I. A., Valente, S. C., and Corval, A.: Decoupling of paired elements, crossover REE patterns, and mirrored spider diagrams: fingerprinting liquid immiscibility in the Tapira alkaline-carbonatite complex, SE Brazil. J. South Am. Earth Sci., 41, 41–56, 2013.
Camerlenghi, A.: Anoxic basins of the eastern Mediterranean: geological framework, Mar. Chem., 31, 1–19, 1990.
Censi, P., Raso, M., Saiano, P., and Zuddas, P.: Differences between Zr and Hf behaviour in oceans in the light of effects induced by atmospheric fallout in marginal basins, Geochim. Cosmochim. Ac., submitted, 2013.
Cita, M. B.: Exhumation of Messinian evaporites in the deep-sea and creation of deep anoxic brine-filled collapsed basins, Sediment. Geol., 188, 357–378, 2006.
De Carlo, E. H. and Green, W. J.: Rare earth elements in the water column of Lake Vanda, McMurdo Dry Valleys, Antarctica, Geochim. Cosmochim. Ac., 66, 1323–1333, 2002.
Dequiedt, S., Saby, N. P. A., Lelievre, M., Jolivet, C., Thioulouse, J., Toutain, B., Arrouays, D., Bispo, A., Lemanceau, P., and Ranjard, L.: Biogeographical patterns of soil molecular microbial biomass as influenced by soil characteristics and management, Glob. Ecol. Biogeogr., 20, 641–652, 2011.
Fee, J. A., Gaudette, H. E., Lyons, W. B., and Long, D. T.: Rare-earth element distribution in Lake Tyrrell groundwaters, Victoria, Australia. Chem. Geol., 96, 67–93, 1992.
Ferrer, M., Werner, J., Chernikova, T. N., Bargiela, R., Fernández, L., La Cono, V., Waldmann, J., Teeling, H., Golyshina, O. V., Glöckner, F. O., Yakimov, M. M., and Golyshin, P. N.: Unveiling microbial life in the new deep-sea hypersaline Lake Thetis, Part II: A metagenomic study, Environ. Microbiol., 14, 268–281, 2012.
Gavrieli, I. and Halicz, L.: Limnological changes in depth distributions of uranium and rare earth elements in a hypersaline brine: the Dead Sea, Israel J. Earth Sci., 51, 243–251, 2002.
Gmelin, H.: Handbuch der anorganische Geochemie, Hf System Nummer 43, Verlag Chemie, Berlin, 1941.
Haley, B. A., Klinkhammer, G. P., and McManus, J.: Rare earth elements in pore waters of marine sediments, Geochim. Cosmochim. Ac., 68, 1265–1279, 2004.

BGD
10, 8977–9002, 2013

Himmler, T., Bach, W., Bohrmann, G., and Peckmann, J.: Rare earth elements in authigenic methane-seep carbonates as tracers for fluid composition during early diagenesis, Chem. Geol., 277, 126–136, 2010.
Hsu, K. J. and Montadert, L.: Initial Reports DSDP, 42, Part 1, US Government Printing Office, Washington, DC, 1249 pp., 1978.
Kučera, J., Cempírek, J., Dolníček, Z., Muchez, P., and Prochaska, W.: Rare earth elements and yttrium geochemistry of dolomite from post-variscan vein-type mineralization of the nízký jeseník and upper silesian basins, czech republic, J. Geochem. Explor., 103, 69–79, 2009.
La Cono, V., Smedile, F., Bortoluzzi, G., Arcadi, E., Maimone, G., Messina, E., Borghini, M., Oliveri, E., Mazzola, S., L'Haridon, S., Toffin, L., Genovese, L., Ferrer, M., Giuliano, L., Golyshin, P. N., and Yakimov, M. M.: Unveiling microbial life in new deep-sea hypersaline Lake Thetis, Part I: Prokaryotes and environmental settings, Environ. Microbiol., 13, 2250–2268, 2011.
Last, F. M., Last, W. M., and Halden, N. M.: Modern and late Holocene dolomite formation: Manito Lake, Saskatchewan, Canada, Sediment. Geol., 281, 222–237, 2012.
Marstorp, H., Guan, X., and Gong, P.: Relationship between dsDNA, chloroform labile C and ergosterol in soils of different organic matter contents and pH, Soil Biol Biochem., 32, 879–882, 2000.
Milliman, J. D., Gastner, M., and Muller, J.: Utilization of magnesium in coralline algae, Geol. Soc. Am. Bull., 82, 573–580, 1971.
Möller, P., Rosenthal, E., Geyer, S., Guttman, J., Dulski, P., Rybakov, M., Zilberbrand, M., Jahnke, C., and Flexer, A.: Hydrochemical processes in the lower Jordan valley and in the Dead Sea area, Chem. Geol., 239, 27–49, 2007.
Monji, A. B., Ahmadi, S. J., and Zolfonoun, E.: Selective biosorption of zirconium and hafnium from acidic aqueous solutions by rice bran, wheat bran and platanus orientalis tree leaves, Separ, Sci. Technol., 43, 597–608, 2008.
Morgan, B., Rate, A. W., Burton, E. D., Smirk, M. N.: Enrichment and fractionation of rare earth elements in FeS- and organic-rich estuarine sediments receiving acid sulfate soil drainage, Chem. Geol., 308–309, 60–73, 2012.
Pierre, C., Ortlieb, L., and Person, A.: Supratidal evaporitic dolomite at Ojo de Liebre lagoon: mineralogical and isotopic arguments for primary crystallization (Baja California, Mexico), J. Sediment. Petrol., 54, 1049–1061, 1984.

BGD
10, 8977–9002, 2013

Pikuta, E. V., Detkova, E. N., Bej, A. K., Marsic, D., and Hoover, R. B.: Anaerobic halo-alkaliphilic bacterial community of athalassic, hypersaline Mono Lake and Owens Lake in California, Proceedings of SPIE – The International Society for Optical Engineering, 4859, 130–144, 2002.

Qu, C. L., Liu, G., and Zhao, Y. F.: Experimental study on the fractionation of yttrium from holmium during the coprecipitation with calcium carbonates in seawater solutions, Geochem. J., 43, 403–414, 2009.

Ranjard, L., Lejon, D., Mougel, C., Scherer, L., Merdinoglu, D., and Chaussod, R.: Sampling strategy in molecular microbial ecology: influence of soil sample size on DNA fingerprinting analysis of fungal and bacterial communities, Environ. Microbiol., 5, 1111–1120, 2003.

Rimoldi, B. and Cita, B. M.: Deep sea turbidites in brine-filled anoxic basins of the Mediterranean Ridge. Depositional madels based on sedimentological and geochemical characteriszation, Rend. Fis. Acc. Lincei, 9, 27–47, 2007.

Ryan, W. F. B. and Hsu, K. J.: Initial Reports DSDP, 13, Part 1, US Government Printing Office, Washington, DC, 514 pp., 1973.

Saager, P. M., Schijf, J., and de Baar, H. J. W.: Trace-metal distributions in seawater and anoxic brines in the eastern Mediterranean Sea, Geochim. Cosmochim. Ac., 57, 1419–1432, 1993.

Sanz-Montero, M. E., Rodríguez-aranda, J. P., and García Del Cura, M. A.: Dolomite-silica stromatolites in miocene lacustrine deposits from the duero basin, spain: the role of organotemplates in the precipitation of dolomite, Sedimentology, 55, 729–750, 2008.

Sanz-Montero, M. E., Rodríguez-Aranda, J. P., and García del Cura, M. A.: Bioinduced precipitation of barite and celestite in dolomite microbialites, examples from Miocene lacustrine sequences in the Madrid and Duero Basins, Spain, Sediment. Geol., 222,138–148, 2009.

Sass, A., Rütters, H., Cypionka, H., and Sass, H.: *Desulfobulbus mediterraneus* sp. nov., a sulfate-reducing bacterium growing on mono- and disaccharides, Archiv. Microbiol., 177, 468–474, 2002.

Schijf, J., De Baar, H. J. W., and Millero, F. J.: Vertical distributions and speciation of dissolved rare earth elements in the anoxic brines of Bannock Basin, eastern Mediterranean Sea, Geochim. Cosmochim. Acta, 59, 3285–3299, 1995.

Smedile, F., Messina, E., La Cono, V., Tsoy, O., Monticelli, L. S., Borghini, M., Giuliano, L., Golyshin, P. N., Mushegian, A., and Yakimov, M. M.: Metagenomic analysis of hadopelagic microbial assemblages thriving at the deepest part of Mediterranean Sea, Matapan-Vavilov Deep, Environ. Microbiol., 15, 167–182, 2013.

BGD
10, 8977–9002, 2013

Stock, A., Breiner, H. W., Pachiadaki, M., Edgcomb, V., Filker, S., La Cono, V., Yakimov, M. M., and Stoeck, T.: Microbial eukaryote life in the new hypersaline deep-sea basin Thetis, Extremophiles, 16, 21–34, 2012.
Takahashi, Y., Chatellier, X., Hattori, K. H., Kato, K., and Fortin, D.: Adsorption of rare earth elements onto bacterial cell walls and its implication for REE sorption onto natural microbial mats, Chem. Geol., 219, 53–67, 2005.
Takahashi, Y., Hirata, T., Shimizu, H., Ozaki, T., and Fortin, D.: A rare earth element signature of bacteria in natural waters?, Chem. Geol., 244, 569–583, 2007.
Takahashi, Y., Yamamoto, M., Yamamoto, Y., and Tanaka, K.: EXAFS study on the cause of enrichment of heavy REEs on bacterial cell surfaces, Geochim. Cosmochim. Ac., 74, 5443–5462, 2010.
Tanaka, K. and Kawabe, I.: REE abundances in ancient seawater inferred from marine limestone and experimental REE partition coefficients between calcite and aqueous solution, Geochem. J. 40, 425–435, 2006.
Taylor, S. R. and McLennan, S. M.: The Geochemical Evolution of the Continental-Crust, Rev. Geophys., 33, 241–265, 1995.
Torfstein, A., Gavrieli, I., and Stein, M.: The sources and evolution of sulfur in the hypersaline Lake Lisan (paleo-Dead Sea), Earth Planet. Sc. Lett., 236, 61–77, 2005.
Tranchida, G., Oliveri, E., Angelone, M., Bellanca, A., Censi, P., D'Elia, M., Neri, R., Placenti, F., Sprovieri, M., Mazzola, S.: Distribution of rare earth elements in marine sediments from the Strait of Sicily (western Mediterranean Sea): evidence of phosphogypsum waste contamination, Mar. Poll. Bull., 62, 182–191, 2011.
Yakimov, M. M., Giuliano, L., Cappello, S., Denaro, R., and Golyshin, P. N.: Microbial community of a hydrothermal mud vent underneath the deep-sea anoxic brine lake Urania (Eastern Mediterranean), Origins Life Evol. B., 37, 177–188, 2007.
Young, R.: The Rietveld Method, International Union of Crystallography, Oxford University Press, Oxford, 1993.
Zhang, F., Xu, H., Konishi, H., Kemp, J. M., Roden, E. E., and Shen, Z.: Dissolved sulfide-catalyzed precipitation of disordered dolomite: implications for the formation mechanism of sedimentary dolomite, Geochim. Cosmochim. Ac., 97, 148–165, 2012.
Zhong, S. J. and Mucci, A.: Partitioning of Rare-Earth Elements (REEs) between Calcite and Seawater Solutions at 25-Degrees-C and 1 Atm, and High Dissolved Ree Concentrations, Geochim. Cosmochim. Ac., 59, 443–453, 1995.

BGD
10, 8977–9002, 2013

Fig. 1. Location of sampling sites.

BGD
10, 8977–9002, 2013

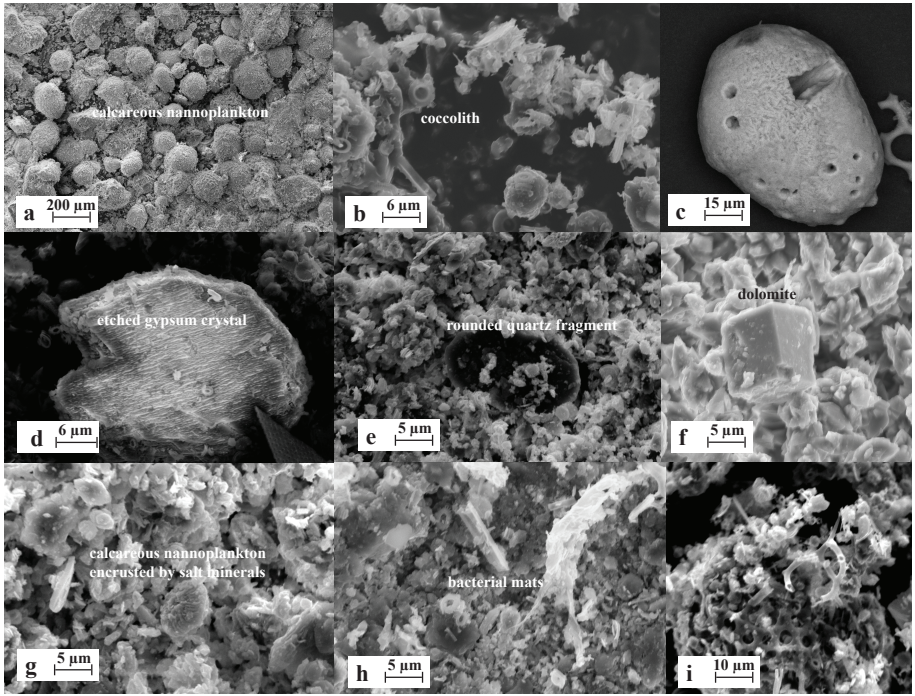

Fig. 2. SEM observations of studied sediments: **(a)**: strong detrital carbonate fraction formed by calcareous nannoplankton; **(b)**: possible effects of microbial activity in sediments; **(c)**: Mg-free detrital calcite, probably from the "Calcare di Base" formation of Messinian age (see typical cubic crystal ghost of halite); **(d)**: etched gypsum crystal showing dissolution figures; **(e)**: rounder quartz grain, probably of aeolic origin, enclosed in fine-grained sediment; **(f)**: fine-rhombohedral dolomite in fine grained sediment; **(f)**: authigenic salt minerals encrusting detrital nannoplankton; **(h)**: possible "organic" textures in sediment; **(i)**: possible "organic" textures in sediment and associated bioclastic materials.

BGD
10, 8977–9002, 2013

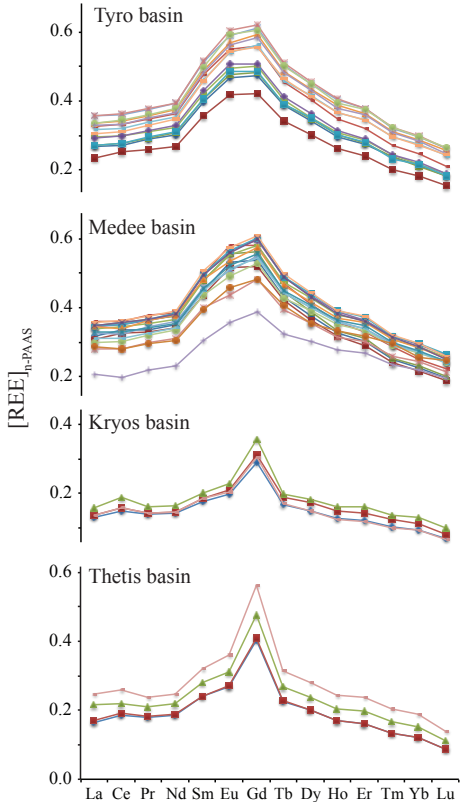

Fig. 3. - Shale-normalized REE patterns of the analysed sediments from different basins. The dashed area represents concentrations measured in carbonate-rich samples from the Tyro basin. Analyses of sediments from the Tyro and Medee basins were carried out on the WS fraction, whereas analyses of sediments from the Kryos and Thetis basins were carried out on the FWSS fraction. For further information see text.

BGD
10, 8977–9002, 2013

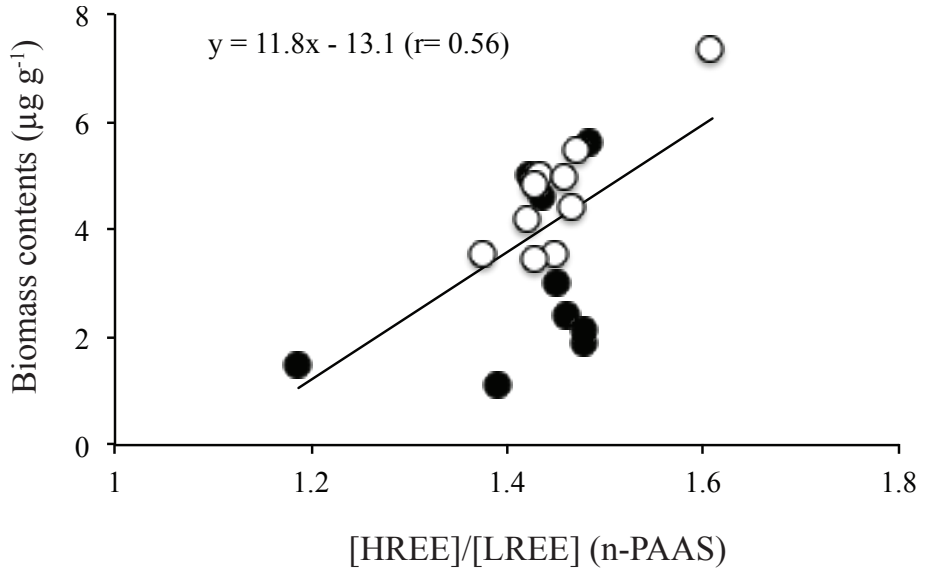

Fig. 4. Relationship between MREE/LREE shale-normalised ratio and biomass contents in sediments from Medee and Tyro basins. Full circles: sediments from the Tyro basin; open circles: sediments from the Medee basin.

BGD
10, 8977–9002, 2013

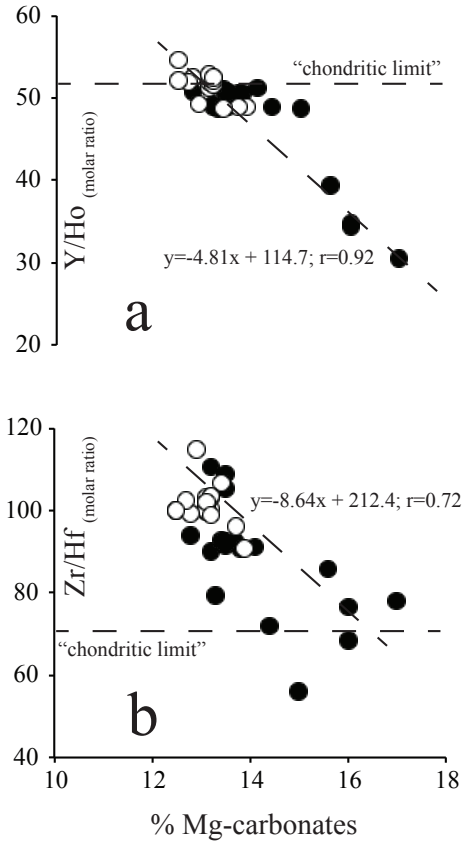

Fig. 5. Relationships between Y/Ho **(a)** and Zr/Hf **(b)** values with respect to the contents of authigenic Mg-carbonates (dolomite + Mg-calcite) in studied assemblages. Symbols as in Fig. 4.

BGD
10, 8977–9002, 2013

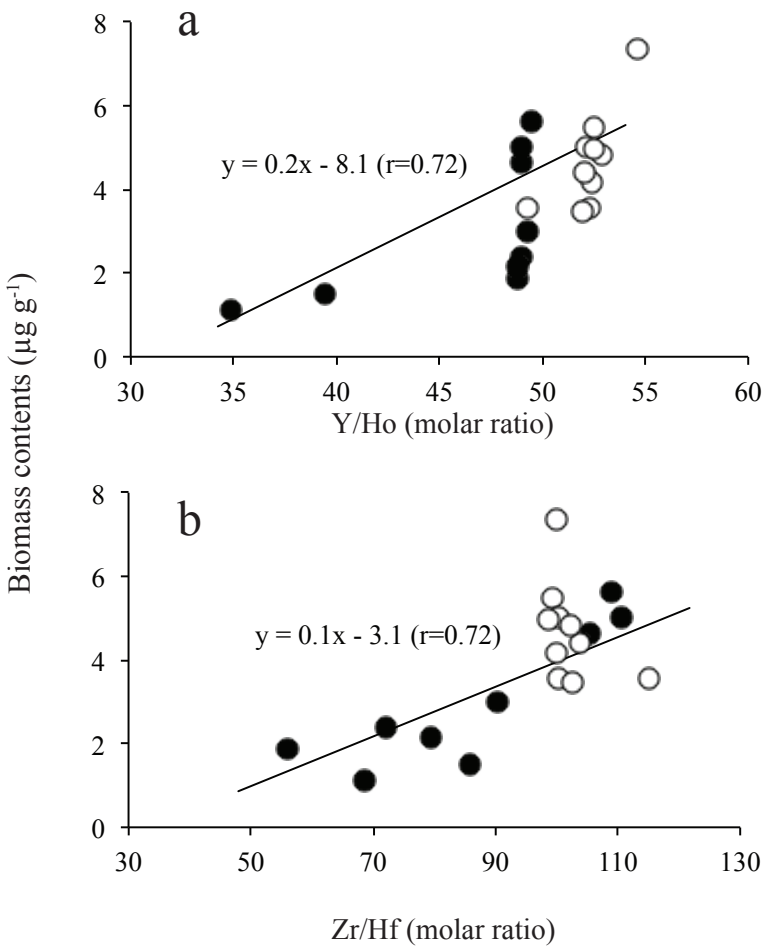

Fig. 6. Relationships between Y/Ho **(a)** and Zr/Hf **(b)** values with respect to the biomass contents in studied assemblages. Symbols as in Fig. 4.

BGD
10, 8977–9002, 2013

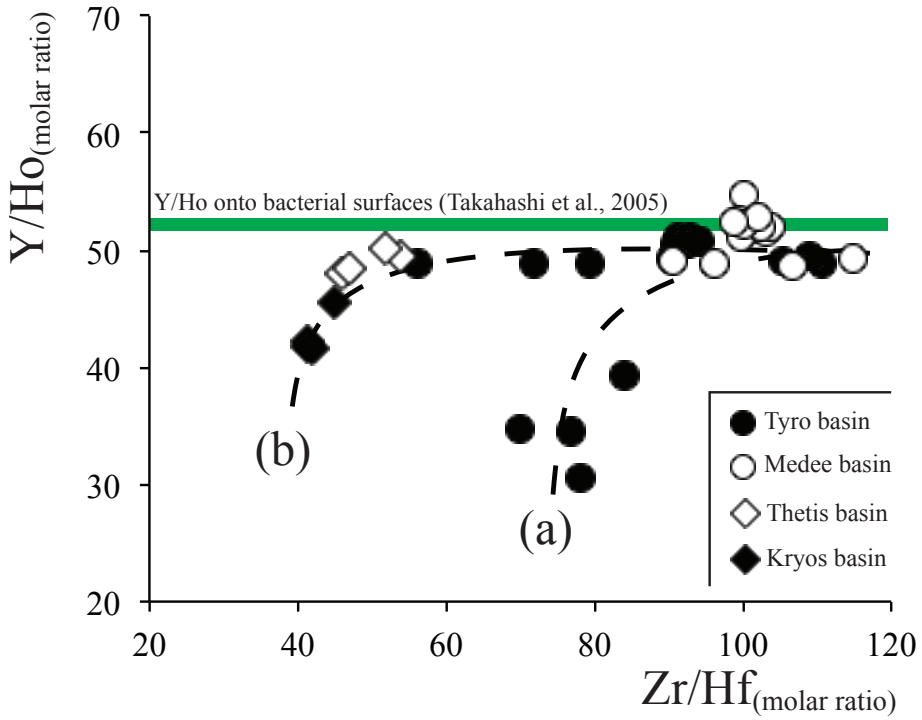

Fig. 7. Y/Ho vs. Zr/Hf behaviour. **(a)** and **(b)** trends represent hypothetical mixing arrays as detailed in the text. The range of Y/Ho values measured onto bacterial surfaces by Takahashi et al. (2005) is reported for reference.

BGD
10, 8977–9002, 2013